Dalton Transactions

Cite this: *Dalton Trans.*, 2012, **41**, 10298

www.rsc.org/dalton

PAPER

Ruthenium amino carboxylate complexes as asymmetric hydrogen transfer catalysts†

Daniel Carmona,* Fernando Viguri,* M. Pilar Lamata, Joaquina Ferrer, Elisa Bardají, Fernando J. Lahoz, Pilar García-Orduña and Luis A. Oro

Received 4th May 2012, Accepted 15th June 2012
DOI: 10.1039/c2dt30976a

The synthesis and characterization of optically active amino carboxylate complexes of formula [(η^6-arene)-Ru(Aa)Cl] (arene = C_6H_6, C_6Me_6, Aa = amino carboxylate) as well as those of the related trimers [{(η^6-arene)Ru(Aa)}$_3$][BF_4]$_3$ are reported. Trimerization takes place with chiral self-recognition: only diastereomers equally configured at the metal, $R_{Ru}R_{Ru}R_{Ru}$ or $S_{Ru}S_{Ru}S_{Ru}$, are detected. The crystal structures of the complexes [(η^6-C_6H_6)Ru(Pip)Cl] and [{(η^6-C_6Me_6)Ru(Pro)}$_3$][BF_4]$_3$ have been determined by X-ray diffraction methods. Both types of complexes catalyse the hydrogen transfer reaction from 2-propanol to ketones with moderate enantioselectivity (up to 68% ee). The enantiodifferentiation achieved can be accounted for by assuming that Noyori's bifunctional mechanism is operating.

Introduction

Asymmetric transfer hydrogenation (ATH) of ketones is a fundamental process for the production of enantiomerically enriched alcohols,[1] which are valuable intermediates for the manufacture of pharmaceuticals and advanced materials.[2] Noyori *et al.* showed that a ruthenium η^6-arene complex containing monotosylated 1,2-diamines could serve as efficient catalyst for the ATH of ketones,[1d,3] operating through a metal–ligand bifunctional mechanism.[4] After this discovery, a variety of new catalytic ruthenium systems have been developed for this process,[1l,m] the best results being obtained when an arene ruthenium(II) moiety is associated with chiral diamines,[1d,5] amino alcohols,[1d–f,i,6] or amino acid derivatives.[7]

On the other hand, L-α-amino acids are inexpensive chiral materials that have been used for the synthesis of optically active transition metal complexes.[8,9] In particular, half-sandwich amino carboxylate complexes, containing d^6 metal ions, such as rhodium(III), iridium(III) or ruthenium(II), have attracted considerable interest in recent years.[9,10] However, the application of amino carboxylate complexes as catalysts for ATH reactions is very limited.[11] In this context, we have reported that (η^5-C_5Me_5)M(III) (M = Rh, Ir) or (η^6-*p*-MeC_6H_4iPr)M(II) (M = Ru, Os) half-sandwich complexes with amino carboxylate ligands[12] efficiently catalyse the ATH of ketonic carbonyl groups.[12d,f–i]

In the present paper, we report on the preparation and characterization of new ruthenium arene complexes of formulae [(η^6-arene)Ru(Aa)Cl] and [{(η^6-arene)Ru (Aa)}$_3$][BF_4]$_3$ (arene = C_6H_6, C_6Me_6), as well as on their application as catalyst precursors for the ATH reaction from 2-propanol to ketones, with the aim of studying the effects of changing the ring substituents on the catalyst while maintaining its half-sandwich structure and the amino carboxylate ligand as a chiral source. Assumption of Noyori's bifunctional mechanism for the ATH reaction explains the sign of the ee obtained.

Results and discussion

Synthesis and characterization of the chloro complexes 1–4

Chloro complexes of formula [(η^6-arene)Ru(Aa)Cl] were obtained by reacting the acetylacetonate compounds [(η^6-arene)-Ru(acac)Cl] (η^6-arene = C_6H_6, C_6Me_6)[13] with stoichiometric amounts of the corresponding L-amino acid (eqn (1)). A schematic representation of these complexes is depicted in Fig. 1.

$$[(\eta^6\text{-arene})\text{Ru(acac)Cl}] + \text{HAa} \rightarrow [(\eta^6\text{-arene})\text{Ru(Aa)Cl}] + \text{Hacac} \quad (1)$$

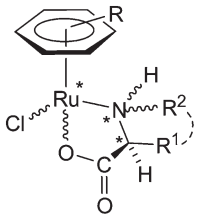

Fig. 1 Schematic representation of the chloro complexes: R = H, R^1 = CH_2Ph, R^2 = Me (**1**); R = H, R^1–R^2 = $(CH_2)_3$ (**2**); R = H, R^1–R^2 = $(CH_2)_4$ (**3**); R = Me_6, R^1–R^2 = $(CH_2)_3$ (**4**).

Instituto de Síntesis Química y Catálisis Homogénea (ISQCH), CSIC – Universidad de Zaragoza, Departamento de Química Inorgánica, Pedro Cerbuna, 12, 50009 Zaragoza, Spain.
E-mail: dcarmona@unizar.es, fviguri@unizar.es

†CCDC 881059 and 881060. For crystallographic data in CIF or other electronic format see DOI: 10.1039/c2dt30976a

Table 1 Diastereomeric composition of complexes **1**–**4**

Complex	Arene	Aa	Molar ratio (a : b)[a]
1a,**b**	C_6H_6	*N*-methyl-L-phenylalaninate (MePhe)	—
2a,**b**	C_6H_6	L-Prolinate (Pro)	—
3a,**b**	C_6H_6	L-piperidine-2-carboxylate (Pip)	85 : 15
4a,**b**	C_6Me_6	Pro	66 : 34

[a] Determined by ^{1}H NMR.

During the formation of these complexes, the metal and the nitrogen atoms become stereogenic centres. Therefore, depending on the configuration they adopt, four diastereomers, namely, R_{Ru},S_C,R_N, S_{Ru},S_C,R_N, R_{Ru},S_C,S_N, S_{Ru},S_C,S_N, can be obtained. However, the new complexes are isolated as mixtures of only two diastereomers, labelled **a** (major) and **b** (minor) (see Table 1). It is well documented[12d,g,i,14] that, from conformational constrains,[15] in half-sandwich complexes containing NO-chelate α-amino carboxylates, the sole configuration adopted by the nitrogen atom is *R* for *N*-methyl-L-phenylalaninates and L-piperidine-2-carboxylates and *S* for L-prolinates. Therefore, most probably, the absolute configuration of the two isomers detected in each case would be R_{Ru},S_C,R_N and S_{Ru},S_C,R_N for the *N*-methyl-L-phenylalaninate **1** and L-piperidine-2-carboxylate **3**, and R_{Ru},S_C,S_N and S_{Ru},S_C,S_N for the L-prolinates **2** and **4** (Fig. 1).

The new complexes were characterized by IR and NMR spectroscopy, elemental analyses (see Experimental section), and by the crystal structure determination, by X-ray diffractometric methods, of compound **3**. The IR spectra showed bands in the 3150–3215 cm^{-1} region (ν(NH))[16] and around 1620 cm^{-1} (ν(CO))[17] compatible with an N,O chelating nature for the amino carboxylate anion. The new complexes are soluble in water but insoluble in common organic solvents such as CH_2Cl_2 or acetone. Complexes **3** and **4** are slightly soluble in CH_3OH and $CHCl_3$, respectively.

The ^{1}H NMR spectrum of complex **1** in D_2O shows more than two sets of signals. In particular, it shows four singlets attributed to C_6H_6 protons at 5.64 (16%), 5.60 (11%), 5.52 (47%), and 5.48 (26%) ppm. Addition of NaCl to the solution produces an increase of the peaks at 5.60 and 5.52 ppm at the expense of the other two. On the other hand, the ^{1}H NMR spectrum of complex **2**, in the same solvent, only shows two C_6H_6 peaks at 5.75 (65%) and 5.66 (35%) ppm. After addition of NaCl, two new C_6H_6 resonances emerge at 5.67 and 5.68 ppm. These spectroscopic data indicate that, in water solution, the chloride ion is partially dissociated in complex **1** and completely dissociated in complex **2** (eqn (2)). Furthermore, as we will see later, the resulting monomeric solvated species rearrange to the trimeric cations formulated in eqn (2). This behaviour prevents the determination of the isomeric composition of isolated complexes **1** and **2**.

$$[(\eta^6\text{-}C_6H_6)Ru(Aa)Cl] \overset{-Cl,D_2O}{\rightleftharpoons} [(\eta^6\text{-}C_6H_6)Ru(Aa)D_2O]^+ \overset{-D_2O}{\rightleftharpoons} 1/3[\{(\eta^6\text{-}C_6H_6)Ru(Aa)\}_3]^{3+} \quad (2)$$

The ^{1}H NMR data of slightly concentrated CD_3OD or $CDCl_3$ solutions of complexes **3** or **4** were consistent with the presence of the η^6-arene group and the amino carboxylate ligand in a 1 : 1 molar ratio. The characterization of these complexes was completed by circular dichroism (CD) and, for complex **3**, by X-ray diffraction studies.

The four complexes are configurationally stable: the composition of diastereomeric mixtures remains essentially unchanged for 7 days, at room temperature, in D_2O (**1**, **2**), CD_3OD (**3**) or $CDCl_3$ (**4**).

Molecular structure of $[(\eta^6\text{-}C_6H_6)Ru(Pip)Cl]$ (3)

Single crystals of complex **3** were grown by slow diffusion of diethyl ether into a methanol solution of an 85 : 15, **3a** : **3b** molar ratio diastereomeric mixture of this compound. The most striking feature of the crystal structure of **3** is the presence of two independent molecules in the asymmetric unit, differing in the configuration at the metal. A molecular representation of the two stereoisomers is depicted in Fig. 2 and selected structural parameters are listed in Table 2. In both independent isomers, the

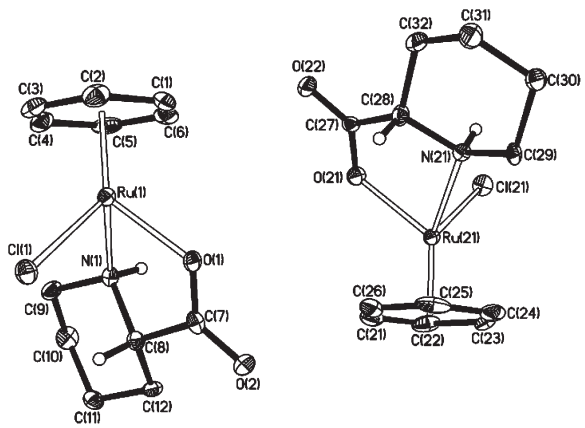

S_{Ru},S_C,R_N-**3b** R_{Ru},S_C,R_N-**3a**

Fig. 2 Molecular representation of both diastereomers in compound **3**. Only hydrogens bonded to the stereogenic centres have been represented.

Table 2 Selected bond lengths (Å) and angles (°) for complex **3**

	Molecule **A**	Molecule **B**
Ru–G[a]	1.650(4)	1.653(4)
Ru–Cl	2.4051(11)	2.4042(11)
Ru–O	2.106(3)	2.096(3)
Ru–N	2.135(3)	2.118(3)
Cl–Ru–G[a]	126.86(16)	128.31(16)
Cl–Ru–O	86.74(8)	87.08(8)
Cl–Ru–N	88.90(9)	81.75(9)
O–Ru–G[a]	130.4(2)	128.6(2)
N–Ru–G[a]	131.0(2)	134.9(2)
O–Ru–N	75.97(11)	77.88(12)

[a] G represents the centroid of the C_6H_6 ring.

asymmetric carbon atoms (C(8) and C(28)) maintain their original *S* configurations, while the nitrogen atom of the aminic group of the L-piperidine-2-carboxylate (N(1) and N(21)) exhibits an *R* configuration. This inverted configuration of the two stereogenic centres of the piperidine ligand has been previously encountered in other [(η^6-arene)M(Pip)Cl] complexes, with (η^5-C_5Me_5)Co[14] or (η^6-*p*-cymene)Os[12g,i] moieties. Therefore, the diastereomers observed in the solid state present the S_{Ru},S_C,R_N (molecule **A**) and R_{Ru},S_C,R_N (molecule **B**) configurations.[18] Although, for half-sandwich complexes, the cocrystallization of two diastereomers differing in the metal configuration has been previously observed,[12a,h,19] single crystals consisting of only one diastereomer is the most common crystallization behaviour for this type of diastereomeric mixtures.

Both independent molecules exhibit analogous structural features. Metal atoms adopt the very well known "three-legged piano-stool" geometry, with an η^6-C_6H_6 group occupying three *fac* positions, while a chlorine atom and the O,N-chelating amino carboxylate ligand complete the coordination sphere of the metals. The bidentate coordination of the amino carboxylate to the ruthenium atom leads to the formation of five-membered Ru–O–C–C–N metallacycles; both metallacycles adopt an envelope E_5 conformation, with similar deviations from planarity, and identical puckering phase values[20] (q = 0.418(3) Å, ϕ = −36.0(5)° and q = 0.386(1) Å, ϕ = −35.4(5)° for molecules **A** and **B**, respectively).

As expected, bond lengths and angles of both diastereoisomers (see Table 2) are rather similar. Both C_6H_6 rings are planar, with an average Ru–C distance of 2.1681(12) Å [range: 2.153(5)–2.184(4) Å], and the Ru to C_6H_6 centroid (G), the Ru–Cl, as well as the Ru–O bond lengths are statistically identical in both diastereomers. The differences between both diastereomers only affect the geometrical parameters involving the coordinated asymmetric N atoms (Ru–N 2.135 *vs.* 2.118(3) Å, or Cl–Ru–N 88.90 *vs.* 81.75(9)°, for instance). The observed Ru–N and Ru–O bond lengths [means 2.126(2) and 2.101(2) Å, respectively], compare well with those found in related [(η^6-arene)Ru(Aa)Cl] complexes (Aa = L-alaninato,[19c] 2.118(6) and 2.089(6) Å; L-serinato, 2.126 and 2.078Å;[21] L-threoninato, 2.122 and 2.048Å).[21] The amino carboxylate bite angles [75.97(11) (**A**) and 77.88(12)° (**B**)] are very similar to that found in the osmium analog[12i] [(η^6-p-cymene)Os(Pip)Cl] (76.26(15)°) and equivalent to those found in the above mentioned Ru complexes (mean 77.8°).

The structural analysis of the spatial arrangement of the coexisting inverted-at-metal diastereomers in [(η^6-arene)Ru(LL*)Cl] half-sandwich complexes has suggested the idea of the existence of a molecular recognition motif, called the "tight inverted piano-stool".[19d] In this packing pattern, H-bond interactions involving Cl and O as acceptor atoms are directly established between both diastereomers. A different situation has been found in complex **3**, where two solvation water molecules interconnect both diastereomers through a hydrogen bonding system leading to a macrocyclic ring described by an $R_2^4(12)$ graphical set (Fig. 3). The crystal cohesion in **3** is then ensured by strong OH···O interactions (see Table 3), between the oxygen atoms of the carboxylate ligands and the water molecules; moreover, NH···O interactions are also observed between these macrocyclic rings.

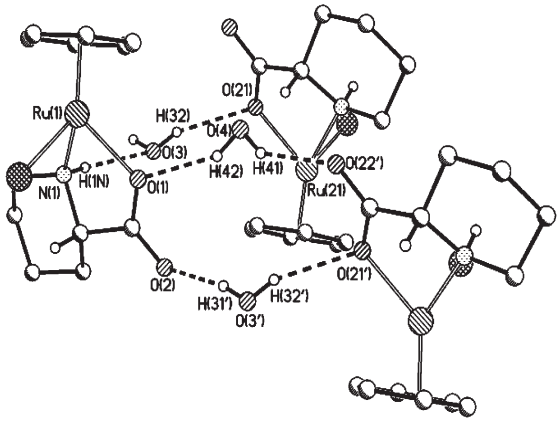

Fig. 3 OH···O hydrogen bond system involving both diastereomers and solvation water molecules. Only H atoms bonded to stereogenic centres as well as those involved in hydrogen bonds have been included. Primed atoms are related to the unprimed ones by a translation along the *b* axis.

Table 3 Selected structural parameters concerning O–H···O bonds (Å and °) for complex **3**

	D–H	D···A	H···A	D–H···A
O(3′)–H(32′)···O(21′)	0.80(2)	3.020(4)	2.26(2)	158(2)
O(3′)–H(31′)···O(2)	0.83(3)	2.752(5)	1.94(3)	168(2)
O(4)–H(42)···O(1)	0.82(4)	2.793(4)	2.06(5)	147(4)
O(4)–H(41)···O(22′)	0.77(6)	2.772(5)	2.00(5)	145(5)
N(1)–H(1N)···O(3)	0.88(5)	3.060(5)	2.21(5)	160(3)

Symmetry code of primed atoms: x, 1 + y, z.

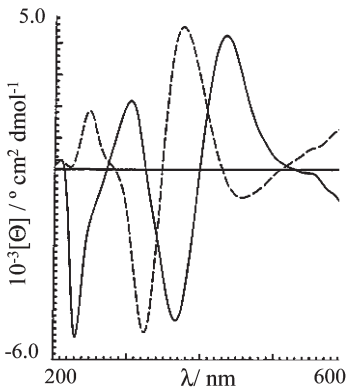

Fig. 4 CD spectra in the 200–600 nm wavelength range: (–) a 85 : 15 molar ratio **3a** : **3b** mixture, (--) a 66 : 34 molar ratio **4a** : **4b** mixture.

Circular dichroism spectra of complexes 3 and 4

The CD spectra of mixtures enriched in the **3a** or **4a** diastereomers are enantiomorphic with respect to each other (Fig. 4). They consist of four maxima around 240, 310, 368, and 440 nm. As no CD transitions have been observed for the parent L-α-amino acids above 230 nm the measured absorptions must be mostly due to metal transitions. Interestingly, the patterns of

the CD spectra of complexes **3** and **4** are comparable to those of the related ruthenium *p*-cymene complexes (R_{Ru},S_C,R_N)-[(η^6-*p*-MeC_6H_4iPr)Ru(Pip)Cl],[12f] and (S_{Ru},S_C,S_N)-[(η^6-*p*-MeC_6H_4iPr)-Ru(Pro)Cl],[12a] respectively. On the basis of this similarity, we assign the R_{Ru} and S_{Ru} configurations for the **a** isomers of compounds **3** and **4**, respectively.

From the conformational constrains above mentioned,[15] the solid molecular structure of complex **3** and the CD measurements we conclude that, in all cases, the isolated isomers are the two possible epimers at the metal and that the absolute configuration of complexes **3** and **4** are R_{Ru},S_C,R_N (**3a**), S_{Ru},S_C,R_N (**3b**) and S_{Ru},S_C,S_N (**4a**), R_{Ru},S_C,S_N (**4b**).

Synthesis and characterization of the cationic trimers 5–8

Treatment of the chloride complexes [(η^6-arene)Ru(Aa)Cl] with equimolar amounts of $AgBF_4$, in methanol, results in the isolation of solids of stoichiometry [(η^6-arene)Ru(Aa)(BF_4)]$_n$·xH_2O (x = 1 or 2) according to analytical and spectroscopic data. As we will show later, these solids contain cationic trimers of formula [{(η^6-arene)Ru(Aa)}$_3$]$^{3+}$ (eqn (3)). A schematic representation of these cations is depicted in Fig. 5.

$$[(\eta^6\text{-arene})\text{Ru(Aa)Cl}] + AgBF_4 \rightarrow 1/3[\{(\eta^6\text{-arene})\text{Ru(Aa)}\}_3][BF_4]_3 + AgCl \quad (3)$$

In spite of the fact that the trimers present nine stereogenic centres, only two diastereomers have been detected in aqueous solution for the four complexes and only one, for complexes **5** and **7**, in acetone (see Table 4). Furthermore, each diastereomer shows only one set of NMR signals and, therefore, within each trimer, the configuration of each threesome of stereogenic centres has to be the same. Formally, the formation of these trimers involves the chloride abstraction by the silver cation from the starting chlorides, giving rise to the corresponding solvated mononuclear species [(η^6-arene)Ru(Aa)(MeOH)]$^+$, followed by the subsequent trimerization of the resulting cationic monomers. In the process, the uncoordinated oxygen of an N,O-coordinated amino carboxylate group displaces the methanol molecule from the coordination sphere of a vecinal [(η^6-arene)Ru(Aa)(MeOH)]$^+$ cation giving rise to a chelate and bridging amino carboxylate ligand. It is interesting to point out that the observed diastereoselectivity in the formation of complexes **5–8** determines that trimerization has to occur with chiral self-recognition among the mononuclear fragments. A similar behaviour has been reported for related d^6 half-sandwich amino carboxylate complexes.[10a,12d,f,g,i,22]

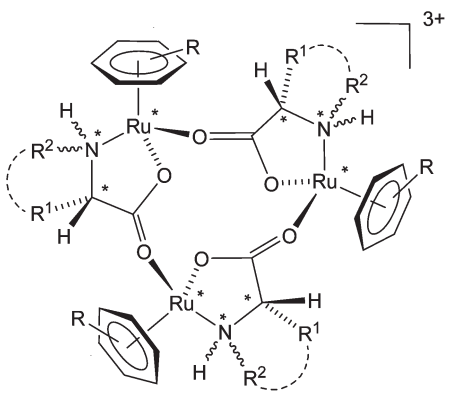

Fig. 5 Schematic representation of the cation of the trimers: R = H, R^1 = CH_2Ph, R^2 = Me (**5**); R = H, R^1–R^2 = $(CH_2)_3$ (**6**); R = H, R^1–R^2 = $(CH_2)_4$ (**7**); R = Me_6, R^1–R^2 = $(CH_2)_3$ (**8**).

Table 4 Diastereomeric composition of complexes **5–8**

Complex	Arene	Aa	Molar ratio (a : b)[a]
5a,**b**	C_6H_6	MePhe	77 : 23[b] (100 : 0)[c]
6a,**b**	C_6H_6	Pro	95 : 5[b,c]
7a,**b**	C_6H_6	Pip	55 : 45[b] (100 : 0)[c]
8a,**b**	C_6Me_6	Pro	72 : 28[b,c]

[a] Determined by ^{1}H NMR. [b] In water. [c] In acetone.

The new complexes have been characterized by IR and NMR spectroscopy, elemental analyses (see Experimental section), and by the determination of the molecular structure of compound **8b** by X-ray diffractometric methods. The IR spectra of the solids showed strong ν(NH) bands in the 3250 cm^{-1} region, the characteristic bands of uncoordinated BF_4 anions under T_d symmetry, and a very strong ν(CO) absorption in the 1565–1575 cm^{-1} range. Reflecting the additional CO coordination, the later is shifted about 50 cm^{-1} to lower energy with respect to the parent chlorides. Moreover, the IR spectra show absorptions in the 3350–3610 cm^{-1} region attributable to crystallized water.

All complexes are soluble in water and acetone, and, as expected, the ^{1}H NMR spectra of complexes **5** and **6** in D_2O, and those measured in the same solvent for the parent chlorides [(η^6-C_6H_6)Ru(MePhe)Cl] (**1**) and [(η^6-C_6H_6)Ru(Pro)Cl] (**2**), are comparable. This equivalence confirms the dissociation equilibrium proposed for the chlorido ligand in eqn (2).

Stereochemical assignments for the complexes have been accomplished through a combination of crystallographic, circular dichroism, and NOE experiments.

Molecular structure of [{(η^6-C_6Me_6)Ru(Pro)}$_3$][BF_4]$_3$ (8b)

Single crystals of this complex were grown by slow diffusion of *n*-hexane into acetone solutions of diastereomeric mixtures of 72 : 28, **8a** : **8b** molar ratio. A molecular representation of the complex is depicted in Fig. 6. The crystal structure consists of trimeric cations [{(η^6-C_6Me_6)Ru(Pro)}$_3$]$^{3+}$ together with BF_4^- counteranions and acetone solvent molecules. Selected structural parameters are summarized in Table 5.

The entire cationic complex of **8b** has crystallographically imposed three-fold symmetry relating the geometrical parameters of the three metal fragments forming the trimer. The amino carboxylate ligand acts as a tridentate chelate and bridging group: the nitrogen and one of the carboxylic oxygen atoms (O(1)) of each amino carboxylate group are bonded to a ruthenium atom in a chelate fashion forming a five-membered metallacycle; the remaining oxygen atom (O(2)) coordinates to a different ruthenium and confers an intermetallic bridging nature to the amino carboxylate ligand. This (*N*,*O*,*O*′)-bridging tridentate proline coordination has been previously reported in

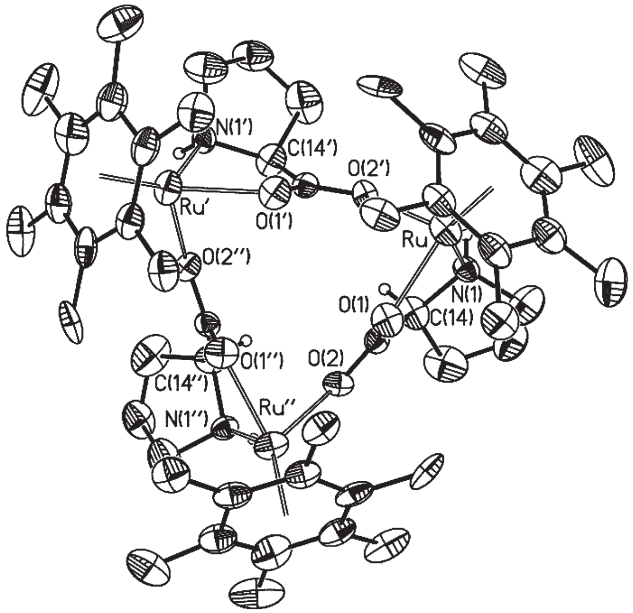

Fig. 6 Molecular representation of the trinuclear cation of **8b**. Only the hydrogen atoms on the stereogenic centres have been included. Primed and double-primed atoms are related to the non-primed ones by the symmetry transformations $1 - y$, $1 + x - y$, z and $-x + y$, $1 - x$, z, respectively.

Table 5 Selected bond lengths (Å) and angles (°) for the trimeric cation of complex **8b**

Ru–G[a]	1.668(10)	Ru–O(2)	2.124(6)
Ru–O(1)	2.137(6)	Ru–N	2.146(7)
G[a]–Ru–O(2)	128.9(4)	O(1)–Ru–O(2)	82.1(3)
G[a]–Ru–O(1)	133.9(4)	O(1)–Ru–N	77.7(3)
G[a]–Ru–N	134.6(4)	O(2)–Ru–N	78.4(3)

[a] G represents the centroid of the ring of the C_6Me_6 arene.

$[\{(\eta^6\text{-}p\text{-}MeC_6H_4iPr)Ru(Pro)\}_3][BF_4]_3$[12d] and $[\{(\eta^6\text{-}p\text{-}MeC_6H_4iPr)Os(Pro)\}_3][BF_4]_3$.[12i] Furthermore, a similar behaviour has been reported for other α-amino acids in trinuclear rhodium[22a] $[\{(\eta^5\text{-}C_5Me_5)Rh(Phe)\}_3]$ $[BF_4]_3$, iridium[12d] $[\{(\eta^5\text{-}C_5Me_5)Ir(Ala)\}_3]$ $[BF_4]_3$ and osmium[12i] $[\{(\eta^6\text{-}p\text{-}MeC_6H_4iPr)Os(Pip)\}_3]$ $[BF_4]_3$ complexes. The five-membered metallacycle Ru–O(1)–C(13)–C(14)–N(1) presents a mixed twist/envelope $^1T_5/^1E$ conformation (Cremer and Pople parameters: q = 0.314(7) Å and $\phi = -13(1)°$).[20]

The metal coordination environments could be described as pseudo-octahedral where, in addition to the three coordination sites occupied by the amino carboxylate donor atoms, an η^6-bonded C_6Me_6 group completes the metal coordination sphere. In such a coordination the metals are stereogenic centres and according to the ligand priority sequence[23] all the metals exhibit *R* configuration. The entire configurational characterization of **8b** also requires the description of the two stereogenic centres of the amino carboxylates; thus, the starting *S* configuration of the asymmetric α-carbon C(14) was not modified along the preparative reaction, while the aminic nitrogen atom also adopts an *S* configuration. The identical configuration of these two atoms (N(1) and C(14)) seems to be correlated due to 'small-fused-ring geometrical restrictions', as it has been already pointed out in other complexes containing pyrrol as a fused ring to the carboxylic function (with only three carbon atoms connecting the amino nitrogen and the carboxylate α-carbon functionalities)[12i] and in related azetidine-2-carboxylate complexes (with only two carbons between nitrogen and α-carbon).[19a] Due to the crystallographically imposed symmetry all of the $\{(\eta^6\text{-}C_6Me_6)Ru(Pro)\}$ moieties are equivalent, and therefore, the absolute configuration of **8b** in the solid state is $R_{Ru}R_{Ru}R_{Ru}S_CS_CS_CS_NS_NS_N$.

The trinuclear core can be described as an equilateral triangle with the arene ligand and the pyrrolidinic cycle of the proline in the external side of the molecule. Therefore, the oxygen atoms (potentially excellent hydrogen-bond acceptors) are located in the internal side of the molecule, which precludes their participation in intermolecular interactions; only a hydrogen bonding interaction is observed between the aminic hydrogen atom (H(1)) and a fluorine atom of the BF_4 anions (N(1)–H(1) 0.930(7), N(1)···F(4) 2.947(12), H(1)···F(4) 2.023(10) Å, and N(1)–H(1)···F(4) 172.3(6)°).

The Ru_3 triangle's edge length in **8b**, 5.585 Å, is longer than the values found in the $\{(\eta^6\text{-}C_6H_4iPr)Ru(Pro)\}_3$ cation (5.268, 5.353 and 5.380 Å). This difference is most probably associated with the bigger size and different electronic properties of the hexamethylbenzene which behaves as a better electron-releasing ligand than *p*-cymene. A comparison of structural parameters in both Ru(Pro) trimer cations shows that the metal weakens its bonding interaction with the chelating donor atoms O(1) and N(1) (2.124(6) and 2.146(7) Å), if compared to the situation reported in $\{(\eta^6\text{-}C_6H_4iPr)Ru(Pro)\}_3$ trimer (Ru–O: 2.096(4), Ru–N: 2.116(5) Å) or in the $\{(\eta^6\text{-}C_6H_6)RuCl(Pro)\}$ monomer (Ru–O: 2.072(2), Ru–N: 2.128(2) Å).[19a]

NMR and circular dichroism spectra of complexes 5–8

Solution stereochemical assignments for these complexes have been accomplished through NOE experiments. Thus, NOE difference spectra for the *N*-methylphenylalaninate complex **5a** in acetone showed enhancement of the signal due to the phenyl protons of the amino carboxylate ligand when the η^6-C_6H_6 protons were irradiated. Moreover, while irradiation of the C*H proton of the same ligand enhances the NMe resonance, no NOE relationship was observed between that proton and the protons of the C_6H_6 ligand. On the other hand, NOE difference spectra for the piperidine-2-carboxylate complex **7a**, showed enhancement of the signal due to the C_6H_6 protons and no NOE effect for the proton bound to the asymmetric carbon atom, while the NH proton was irradiated. These NOE data are only compatible with R_{Ru},S_C,R_N configurations for complexes **5a** and **7a** (Fig. 7).

With respect to the prolinate compounds, for complex **6a**, NOE difference spectra in acetone showed enhancement of the signal due to the η^6-C_6H_6 protons when the *pro-S* NCH_2 proton[24] was irradiated (Fig. 8), but no NOE relationship was observed between the same aromatic protons and the C*H proton. However, for complex **8a**, NOE was observed between the η^6-C_6Me_6 protons and both the C*H and NH protons. In both complexes, irradiation of the NH proton enhances the C*H resonance. These NOE data indicate that complexes **6a** and

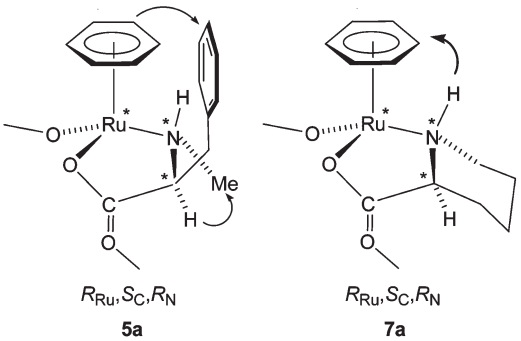

Fig. 7 Selected NOE for **5a** and **7a** (only one monomer and the bridging oxygen are shown).

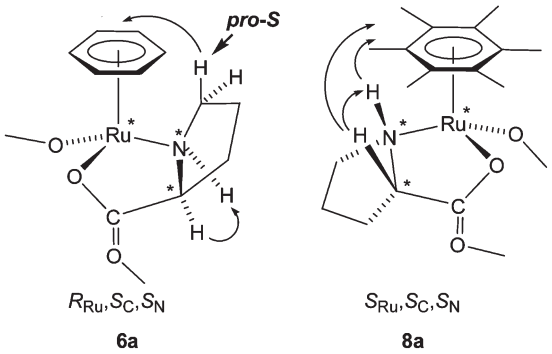

Fig. 8 Selected NOE for **6a** and **8a** (only one monomer and the bridging oxygen are shown).

8a present R_{Ru},S_C,S_N and S_{Ru},S_C,S_N configurations, respectively (Fig. 8).

Among the series of ruthenium trimers, the metal configuration can also be inferred from the solution chiroptical properties. Thus, the CD spectra of pure **5a** and **7a** and of a diastereomeric mixture of complex **6**, enriched in the **6a** isomer, consisted of two maxima in the 350–355 and 415–420 nm ranges, both with positive Cotton effects. The CD spectrum of a mixture enriched in **8a** clearly shows a pseudoenantiomorphic relationship to the trimers **5a**, **6a**, and **7a**, since a similar morphology but opposite Cotton effects were observed (see Experimental section). As the CD spectra of the parent L-amino acids are silent above 230 nm, we assume that the measured absorptions are mostly due to metal transitions. These observations allow us to assign an opposite configuration at ruthenium for isomer **8a** with respect to isomers **5a–7a**, in good agreement with the NMR data discussed above.

On the other hand, the substitution on the η^6-arene ligand seems to exert a significant influence on the configuration at the metal of the trimers. Thus, while for the benzene and *p*-cymene derivatives $[\{(\eta^6\text{-}C_6H_6)Ru(Pro)\}_3][BF_4]_3$ (**6**) and $[\{(\eta^6\text{-}p\text{-}MeC_6H_4iPr)Ru(Pro)\}_3][BF_4]_3$ (**9**)[12d] in the thermodynamically preferred diastereomer the configuration at ruthenium is *R*, for the hexamethylbenzene analogue $[\{(\eta^6\text{-}C_6Me_6)Ru(Pro)\}_3][BF_4]_3$ (**8**) the *S* configuration at the metal gives the most stable isomer.

Finally, all the four trimers **5–8** are configurationally stable, for days at room temperature, in water or acetone solution.

Table 6 Asymmetric transfer hydrogenation[a] of acetophenone

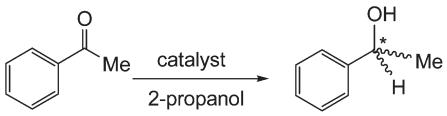

Entry	Complex	Config. at N	Conv. (%)[b]	ee (%)
1	$[(\eta^6\text{-}C_6H_6)Ru(MePhe)Cl]$ (**1**)[c]	*R*	40	20 (*S*)
2	$[\{(\eta^6\text{-}C_6H_6)Ru(MePhe)\}_3]^{3+}$ (**5**)	*R*	53	22 (*S*)
3	$[(\eta^6\text{-}C_6H_6)Ru(Pro)Cl]$ (**2**)[c]	*S*	74	45 (*R*)
4	$[\{(\eta^6\text{-}C_6H_6)Ru(Pro)\}_3]^{3+}$ (**6**)	*S*	64	47 (*R*)
5	$[(\eta^6\text{-}C_6H_6)Ru(Pip)Cl]$ (**3**)[c]	*R*	87	41 (*S*)
6	$[\{(\eta^6\text{-}C_6H_6)Ru(Pip)\}_3]^{3+}$ (**7**)	*R*	98	39 (*S*)
7	$[(\eta^6\text{-}C_6Me_6)Ru(Pro)Cl]$ (**4**)	*S*	90	43 (*R*)
8	$[\{(\eta^6\text{-}C_6Me_6)Ru(Pro)\}_3]^{3+}$ (**8**)	*S*	96	46 (*R*)

[a] Reaction conditions: all reactions were carried out at 83 °C. Catalyst 0.01 mmol in 5 mL of 2-propanol; molar ratio catalyst–HCOONa–acetophenone: 1 : 2 : 100. [b] Conversion, determined by gas chromatography, after one hour of reaction. [c] Molar ratio 1 : 1 : 100.

Asymmetric hydrogen transfer reactions

We have tested the new ruthenium amino carboxylate complexes **1–8** as catalyst precursors for the ATH reaction from 2-propanol to ketones. Reactions have been carried out at 83 °C, in the presence of the mild base HCOONa, with catalyst–base–substrate molar ratios of 1 : 1 : 100 or 1 : 2 : 100. Both conversion and enantioselectivity have been determined by gas chromatography. Table 6 collects a selection of the results obtained in the reduction of acetophenone. Under the standard conditions, 40 to 98% conversion of the starting material can be achieved, in one hour of reaction, to yield 1-phenylethanol with up to 47% ee. Neutral chloride complexes and cationic trimers containing the same amino carboxylate ligand showed similar enantiomeric excesses (compare entries 1 and 2, 3 and 4, 5 and 6, and 7 and 8). Probably, the active catalytic species originate through a common intermediate, namely, $[(\eta^6\text{-arene})Ru(Aa)(iPrOH)]^+$, formed by halogen abstraction from the chlorides or by cleavage of the Ru–O(bridging) bond from the trimers and, therefore, both catalyst precursors behave similarly in the ATH reaction.

With respect to the enantioselectivity of the process, catalysts based on the cyclic aminocarboxylates Pro or Pip (entries 3–8) produced better enantioselectivity than those based on the linear one MePhe (entries 1 and 2). The greater conformational rigidity of the former could account for the measured increment in ee. However, the most striking result is that while prolinate compounds give the *R* alcohol (entries 3, 4, 7, and 8), *N*-methylphenylalaninates (entries 1 and 2) and piperidine-2-carboxylates (entries 5 and 6) preferentially afford the *S* alcohol. This change of sign in the enantioselection can be explained assuming that the bifunctional concerted mechanism of Noyori[4a] is operating in our catalytic system (Scheme 1). According to it, from the starting 2-propanol intermediate $[(\eta^6\text{-arene})Ru(Aa)(iPrOH)]^+$, a ruthenium hydride is formed by β-elimination and, in the key step of this mechanism, the Ru–H and the N–H protons are simultaneously transferred from the catalyst to the ketone carbonyl group *via* the six-membered transition state depicted in Scheme 1. In our case, this cyclic intermediate can only be built

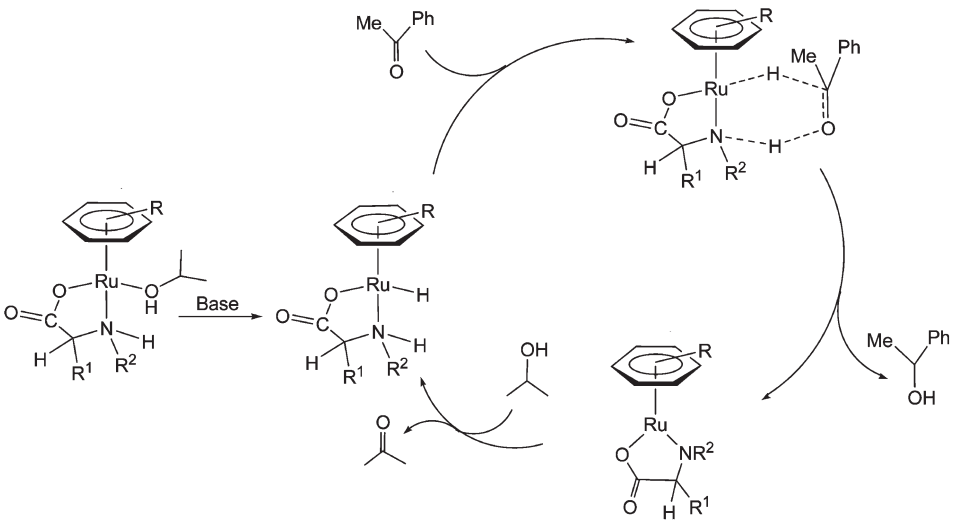

Scheme 1 Asymmetric transfer reaction catalysed by amino carboxylate Ru compounds.

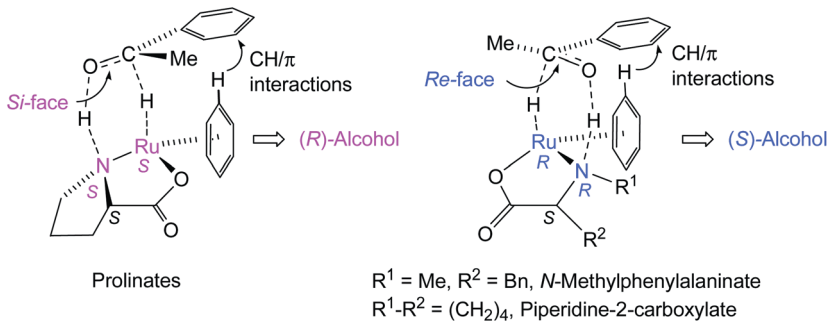

Fig. 9 Proposed active intermediates for the ATH reaction.

up when the metal and the nitrogen adopt the same configuration (Fig. 9) and, therefore, only the S_{Ru},S_C,S_N isomers for the prolinate complexes and the R_{Ru},S_C,R_N isomers for the piperidine-2-carboxylate and *N*-methylphenylalaninate compounds can be active catalysts for the attempted ATH process. Enantioselection occurs because CH/π interactions between the hydrogen atoms on the η^6-coordinated arene and the phenyl ring of the acetophenone[4b,c] fix the ketone enantioface through which the Ru–H and N–H protons are released from the catalyst to the C=O bond (Fig. 9). The experimental stereochemical outcome is in good agreement with this mechanistic proposal.

Next, we studied the reduction of some phenyl substituted acetophenones using as catalyst precursors the prolinate complexes **2** and **4** as well as the related *p*-cymene complex [(η^6-*p*-MeC_6H_4iPr)Ru(Pro)Cl] (**9**) recently reported by us.[12d] Table 7 lists the most representative results together with the reaction conditions. For comparative purposes we also include in Table 7 the results obtained for acetophenone (entries 1–3).

In general good conversions are achieved after one hour of treatment under the conditions indicated in Table 7, with moderate enantioselectivity. No obvious relationship can be encountered between the nature of the substituents and either rate or selectivity. For all the ketones investigated, the ee decreases when benzene or hexamethylbenzene is used as the ligand instead of *p*-cymene.

Conclusions

Half-sandwich complexes of the type [(η^6-arene)Ru(Aa)Cl] that incorporate chiral amino carboxylate ligands are easily prepared from the corresponding acetylacetonate complex [(η^6-arene)Ru(acac)Cl] as a mixture of epimers at the metal. Abstraction of the chloride affords the new trinuclear amino carboxylate cationic complexes [{(η^6-arene)Ru(Aa)}$_3$](BF$_4$)$_3$. Trimerizations take place with self-recognition: only trimers with the same configuration at the three metal atoms are obtained. Mononuclear and trinuclear complexes are effective catalysts for the enantioselective reduction of prochiral ketones by hydrogen transfer from 2-propanol. Assumption of Noyori's mechanism for the ATH reaction allows us to explain the sign of the ee obtained.

Experimental

All solvents were dried over appropriate drying agents, distilled under nitrogen and degassed prior to use. All preparations have

Table 7 Asymmetric transfer hydrogenation[a] of other ketones

Entry	Complex	Ketone	Conv.[b] (%)	ee (%)
1	[(η^6-C_6H_6)Ru(Pro)Cl] (**2**)	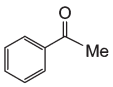	74	45 (*R*)
2	[(η^6-C_6Me_6)Ru(Pro)Cl] (**4**)[c]		90	43 (*R*)
3	[(η^6-*p*-MeC_6H_4iPr)Ru(Pro)Cl] (**9**)		88	67 (*R*)
4	[(η^6-C_6H_6)Ru(Pro)Cl] (**2**)	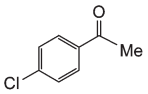	72	24 (*R*)
5	[(η^6-C_6Me_6)Ru(Pro)Cl] (**4**)[c]		50	30 (*R*)
6	[(η^6-*p*-MeC_6H_4iPr)Ru(Pro)Cl] (**9**)		95	46 (*R*)
7	[(η^6-C_6H_6)Ru(Pro)Cl] (**2**)	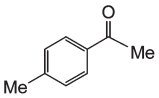	55	35 (*R*)
8	[(η^6-C_6Me_6)Ru(Pro)Cl] (**4**)[c]		52	34 (*R*)
9	[(η^6-*p*-MeC_6H_4iPr)Ru(Pro)Cl] (**9**)		80	50 (*R*)
10	[(η^6-C_6H_6)Ru(Pro)Cl] (**2**)	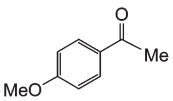	8	39 (*R*)
11	[(η^6-C_6Me_6)Ru(Pro)Cl] (**4**)[c]		12	57 (*R*)
12	[(η^6-*p*-MeC_6H_4iPr)Ru(Pro)Cl] (**9**)		59	68 (*R*)

[a] Reaction conditions: all reactions were carried out at 83 °C; catalyst 0.01 mmol in 5 mL of 2-propanol; molar ratio catalyst–HCOONa–ketone: 1 : 1 : 100. [b] Determined by gas chromatography, after one hour of reaction. [c] Molar ratio: 1 : 2 : 100.

been carried out under nitrogen. Infrared spectra were obtained as Nujol mulls with a Perkin-Elmer 1330 spectrophotometer. Carbon, hydrogen, and nitrogen analyses were performed using a Perkin-Elmer 240 B microanalyzer. ^{1}H NMR spectra were recorded on a Varian UNITY 300 spectrometer (299.95 MHz) or a Bruker 300 ARX (300.10 MHz). Chemical shifts are expressed in ppm upfield from $SiMe_4$. CD spectra were determined in a 1 cm path length cell by using a Jasco-710 apparatus at concentrations of approximately 5×10^{-4} mol L^{-1}. NOEDIFF spectra were obtained using standard procedures. Gas chromatography was performed on a Hewlet-Packard 3398 gas chromatograph equipped with a split-mode capillary injection system and flame ionization detector, using a CP-Cyclodex-B 236M 25 m × 0.25 mm × 0.25 μm film column.

Preparation of [(η^6-C_6H_6)Ru(Aa)Cl] (1–3)

To a solution of [(η^6-C_6H_6)Ru(acac)Cl] (300.0 mg, 0.95 mmol) in methanol (20 mL) the appropriate amino acid (0.95 mmol) was added. The resulting solutions were stirred for 24 h. During this time the precipitation of a yellow solid was observed. The solid was filtered off, washed with methanol and air-dried.

Complex 1. Yield: 84%. Anal. Calcd for $C_{16}H_{18}NClO_2Ru$: C, 48.9; H 4.6; N, 3.6. Found: C, 49.1; H, 4.7; N, 3.5. IR (Nujol, cm^{-1}): ν(NH) 3215 (m), ν(CO) 1633 (s). ^{1}H NMR (D_2O): four species in 47 : 26 : 16 : 11 molar ratio were detected: δ 3.16 (s, 3H, Me), 3.56 (m, 1H, CHCOO), 5.52 (s, 6H, C_6H_6), 7.07–7.36 (m, Ph) (47%); 2.59 (s, 3H, Me), 5.48 (s, 6H, C_6H_6) (26%); 2.70 (s, 3H, Me), 5.64 (s, 6H, C_6H_6), (16%); 3.09 (s, 3H, Me), 5.60 (s, 6H, C_6H_6) (11%).

Complex 2. Yield: 92%. Anal. Calcd for $C_{11}H_{14}NClO_2Ru$: C, 40.2; H 4.3; N, 4.3. Found: C, 40.0; H, 4.2; N, 4.2. IR (Nujol, cm^{-1}): ν(NH) 3162 (m), ν(CO) 1614 (s). ^{1}H NMR (D_2O): two species in 65 : 35 molar ratio were detected: δ 1.58, 1.88, 2.10 (m, 4H, CH_2), 3.17 (m, 1H, CHCOO), 3.17 (m, 1H, *pro-S* NCH_2), 3.33 (m, 1H, *pro-R* NCH_2), 3.93 (m, 1H, NH), 5.75 (s, 6H, C_6H_6) (65%); 2.5 m, 3.15 (m, 1H, *pro-R* NCH_2), 3.60 m, 5.66 (s, 6H, C_6H_6) (35%).

Complex 3. Yield: 80%, **3a** : **3b** molar ratio, 85 : 15. Anal. Calcd for $C_{12}H_{16}NClO_2Ru$: C, 42.05; H 4.7; N, 4.1. Found: C, 42.1; H, 4.7; N, 4.0. IR (Nujol, cm^{-1}): ν(NH) 3174 (m), ν(CO) 1643 (s). CD (CH_3OH), **3a** : **3b** molar ratio, 85 : 15, [Θ]λ values of maxima and nodes (λ, nm): −5200 (230), 0 (270), +2200 (300), 0 (325), −4800 (365), 0 (400), +4150 (430). **3a**: ^{1}H NMR (CD_3OD): δ 1.35–3.20 (m, 8H, CH_2), 3.65 (m, 1H, CHCOO), 5.69 (s, 6H, C_6H_6). **3b**: ^{1}H NMR (CD_3OD): δ 5.75 (s, 6H, C_6H_6).

Preparation of [(η^6-C_6Me_6)Ru(Pro)Cl] (4)

To a solution of [(η^6-C_6Me_6)Ru(acac)Cl] (401.3 mg, 1.01 mmol) in methanol (20 mL), L-Proline (122.7 mg, 1.06 mmol) was added. The resulting solution was stirred for 24 h and then filtered through Kieselguhr to eliminate any solid residue. After partial concentration under reduced pressure, the slow addition of diethyl ether gave a hygroscopic orange solid which was washed with diethyl ether and vacuum-dried.

Complex 4. Yield: 75%, **4a** : **4b** molar ratio, 66 : 34. Anal. Calcd for $C_{17}H_{26}NClO_2Ru{\cdot}2H_2O$: C, 45.5; H 6.7; N, 3.1. Found: C, 45.2; H, 6.6; N, 3.0. IR (Nujol, cm^{-1}): ν(OH) 3593 (m), ν(NH) 3200 (m), ν(CO) 1605 (s). CD ($CHCl_3$), **4a** : **4b** molar ratio, 66 : 34, [Θ]λ values of maxima and nodes (λ, nm): +1800 (250), 0 (280), −5200 (320), 0 (345), +4600 (370), 0 (420), −800 (450). **4a**: ^{1}H NMR ($CDCl_3$): δ 2.13 (s, 18H, C_6Me_6), 6.60 (m, 1H, NH). **4b**: ^{1}H NMR ($CDCl_3$): δ 2.17 (s, 18H, C_6Me_6), 6.14 (m, 1H, NH).

Preparation of $[\{(\eta^6\text{-}C_6H_6)Ru(Aa)\}_3][BF_4]_3$ (5–7)

To a solution, in acetone–water (v/v, 90 : 10), of the corresponding $[(\eta^6\text{-}C_6H_6)Ru(Aa)Cl]$ compound (0.58 mmol), $AgBF_4$ (118.2 mg, 0.60 mmol) was added. The mixture was stirred for 1 h, in the absence of light, and the precipitated AgCl was filtered off. The filtrate was evaporated to dryness and the resulting yellow solid was recrystallized from acetone–*n*-hexane.

Complex 5. Yield: 73%, **5a** : **5b** molar ratio, 77 : 23. Anal. Calcd for $C_{48}H_{54}B_3F_{12}N_3O_6Ru_3{\cdot}3H_2O$: C, 41.6; H 4.4; N, 3.0. Found: C, 42.0; H, 4.3; N, 2.9. IR (Nujol, cm^{-1}): ν(OH) 3606 (m), ν(NH) 3248 (m), ν(CO) 1575 (s), $\nu(BF_4)$ 1060 (s), 521 (m). CD ($(CH_3)_2CO$), **5a** : **5b** molar ratio, 77 : 23, $[\Theta]\lambda$ values of maxima, (λ, nm): +20 000 (350), +31 000 (420). **5a**: ^{1}H NMR (D_2O): δ 2.55 (bs, 3H, Me), 2.97 (m, 2H, CH_2), 2.82 (m, 1H, CHCOO), 5.48 (s, 6H, C_6H_6), 7.00–7.40 (m, Ph). **5b**: ^{1}H NMR (D_2O):δ 3.13 (bs, 3H, Me), 5.64 (s, 6H, C_6H_6). **5a**: ^{1}H NMR ($(CD_3)_2CO$): δ 2.22 (m, 1H, CHCOO), 2.56 (d, J_{HH} = 5.6 Hz, 3H, Me), 2.97 (dd, 1H, AB part of an ABX system, J_{AB} = 15.1 Hz, J_{AX} = 4.4 Hz, C*H*H), 3.13 (dd, 1H, AB part of an ABX system, J_{BX} = 8.1 Hz, CH*H*), 6.14 (s, 6H, C_6H_6), 6.42 (m, 1H, NH), 7.10–7.35 (m, Ph).

Complex 6. Yield: 82%, **6a** : **6b** molar ratio, 95 : 5. Anal. Calcd for $C_{33}H_{42}B_3F_{12}N_3O_6Ru_3{\cdot}3H_2O$: C, 33.2; H 4.05; N, 3.5. Found: C, 33.0; H, 4.0; N, 3.5. IR (Nujol, cm^{-1}): ν(OH) 3607 (m), ν(NH) 3262 (m), ν(CO) 1583 (s), $\nu(BF_4)$ 1051 (s), 522 (m). CD ($(CH_3)_2CO$), **6a** : **6b** molar ratio, 95 : 5, $[\Theta]\lambda$ values of maxima, (λ, nm): +20 000 (355), +32 000 (420). **6a**: ^{1}H NMR (D_2O): δ 1.55, 1.84, 2.07 (m, 4H, CH_2), 3.17 (m, 1H, CHCOO), 3.17 (m, 1H, *pro-S* NCH_2), 3.96 (m, 1H, *pro-R* NCH_2), 5.60 (m, 1H, NH), 5.75 (s, 6H, C_6H_6). **6b**: ^{1}H NMR (D_2O) δ 5.66 (s, 6H, C_6H_6). **6a**: ^{1}H NMR ($(CD_3)_2CO$): δ 1.6–2.3 (m, 4H, CH_2), 3.28 (m, 1H, CHCOO), 3.49 (m, 1H, *pro-S* NCH_2), 4.27 (m, 1H, *pro-R* NCH_2), 5.60 (m, 1H, NH), 6.18 (s, 6H, C_6H_6). **6b**: ^{1}H NMR ($(CD_3)_2CO$): δ 6.14 (s, 6H, C_6H_6).

Complex 7. Yield: 85%, **7a** : **7b** molar ratio, 55 : 45. Anal. Calcd for $C_{36}H_{48}B_3F_{12}N_3O_6Ru_3{\cdot}3H_2O$: C, 35.0; H 4.4; N, 3.4. Found: C, 35.2; H, 4.3; N, 3.3. IR (Nujol, cm^{-1}): ν(OH) 3606 (m), ν(NH) 3230 (m), ν(CO) 1574 (s), $\nu(BF_4)$ 1066 (s), 522 (m). CD ($(CH_3)_2CO$), **7a** : **7b** molar ratio, 55 : 45, $[\Theta]\lambda$ values of maxima, (λ, nm): +20 000 (355), +39 000 (4150. **7a**: ^{1}H NMR (D_2O): δ 3.75 (m, 1H, CHCOO), 6.63 (m, 1H, NH), 5.72 (s, 6H, C_6H_6). **7b**: ^{1}H NMR (D_2O): δ 3.87 (m, 1H, CHCOO), 5.75 (s, 6H, C_6H_6). **7a**: ^{1}H NMR ($(CD_3)_2CO$): δ 1.3–2.0 (m, 6H, CH_2), 2.34 (m, 1H, CHCOO), 2.90 (m, 1H, *pro-S* NCH_2), 4.00 (m, 1H, *pro-R* NCH_2), 6.11 (s, 6H, C_6H_6), 6.31 (m, 1H, NH).

Preparation of $[\{(\eta^6\text{-}C_6Me_6)Ru(Pro)\}_3][BF_4]_3$ (8)

To a solution of $[(\eta^6\text{-}C_6Me_6)Ru(acac)Cl]$ (308.8 mg, 0.78 mmol) in methanol (20 mL), L-Proline (95.3 mg, 0.82 mmol) was added. The solution was stirred for 24 h and then filtered through Kieselguhr to eliminate any solid residue. $AgBF_4$ (155.6 mg, 0.79 mmol) was added to the resulting solution, the mixture was stirred for 1 h in the absence of light and then the precipitated AgCl was filtered off. The filtrate was evaporated to dryness, and the resulting yellow solid was recrystallized from acetone–*n*-hexane.

Complex 8. Yield: 77%, **8a** : **8b** molar ratio, 72 : 28. Anal. Calcd for $C_{51}H_{78}B_3F_{12}N_3O_6Ru_3{\cdot}6H_2O$: C, 40.8; H 6.0; N, 2.8. Found: C, 40.5; H, 5.9; N, 2.9. IR (Nujol, cm^{-1}): ν(OH) 3604 (m), ν(NH) 3200 (m), ν(CO) 1574 (s), $\nu(BF_4)$ 1061 (s), 521 (m). CD ($(CH_3)_2CO$), **8a** : **8b** molar ratio, 72 : 28, $[\Theta]\lambda$ values of maxima, (λ, nm): −16 000 (330), −10 000 (435). **8a**: ^{1}H NMR (D_2O): δ 2.02 (s, 18H, C_6Me_6). **8b**: ^{1}H NMR (D_2O): δ 1.92 (s, 18H, C_6Me_6). **8a**: ^{1}H NMR ($(CD_3)_2CO$): δ 1.4–2.6 (m, 4H, CH_2), 2.42 (s, 18H, C_6Me_6), 3.85 (m, 1H, CHCOO), 4.00 (m, 1H, *pro-S* NCH_2), 4.25 (m, 1H, *pro-R* NCH_2), 5.20 (m, 1H, NH). **8b**: ^{1}H NMR ($(CD_3)_2CO$): δ 2.38 (s, 18H, C_6Me_6).

Transfer hydrogenation experiments

Catalyst (0.01 mmol metal), HCOONa (0.01–0.02 mmol, aqueous solution), and 2-propanol (4 mL) were mixed under nitrogen at room temperature in a flask which was then equipped with a reflux condenser and immersed in an oil bath at 83 °C. To the boiling solution, the ketone (1 mmol) was added in 1 mL of 2-propanol. Reactions were monitored by gas-liquid chromatography and the products were identified by their retention times compared to those of the literature.[3b,7a,25]

Crystal structure determinations

X-ray diffraction data were collected at 100(2) K with graphite-monochromated MoK_α radiation (λ = 0.71073 Å) using narrow ω rotation (0.3°) on a Bruker SMART APEX CCD area detector diffractometer. Intensities were integrated and corrected for absorption effects with SAINT-PLUS program.[26] The structures were solved by direct methods with SHELXS-97.[27] Refinement, by full-matrix least-squares on F^2, was performed with SHELXL-97.[28] Anisotropic displacement parameters were included for all non-solvent non-H atoms. Most of the hydrogen atoms were included in calculated positions and refined with displacement and positional riding parameters. In all the structures, additionally to the internal configuration reference of the α-asymmetric carbon of the amino acid, the Flack parameter was refined as a check on the correct absolute structure determination.[29] Particular details concerning the presence of solvent, static disorder and specific refinements are listed below.

Crystal data for 3. $C_{12}H_{16}ClNO_2Ru{\cdot}H_2O$, M = 360.80; yellow needle, 0.377 × 0.074 × 0.030 mm^3; monoclinic, $C2$; a = 17.365(2) Å, b = 6.2660(9) Å, c = 24.847(3) Å; β = 106.045(2)°; Z = 8; V = 2598.2(6) Å^3; D_c = 1.845 g cm^{-3}; μ = 1.412 mm^{-1}, min. and max. transmission factors 0.758 and 0.846; $2\theta_{max}$ = 56.78°; 8590 collected reflections, 5562 unique [R_{int} = 0.017]; number of data/restraints/parameters 5562/3/357; final GoF 1.015; R_1 = 0.0296 [5275 reflections, $I > 2\sigma(I)$]; wR_2 = 0.0674 for all data; Flack parameter x = −0.02(3); largest difference peak 0.84 e Å^{-3}. The hydrogen atoms of the stereogenic centers (nitrogen and α-carbon of the amino acid) have been included in the model in observed positions and freely refined. Hydrogen atoms of water molecules have been observed, and refined with a restraint in OH distances.

Crystal data for 8b. $C_{51}H_{78}B_3F_{12}N_3O_6Ru_3{\cdot}3(C_3H_6O)$, M = 1567.04; orange prism, 0.352 × 0.137 × 0.129 mm^3; hexagonal, $P6_3$; $a = b$ = 19.161(3) Å, c = 10.4784(14) Å; Z = 2; V = 3331.6(8) Å^3; D_c = 1.562 g cm^{-3}; μ = 0.76 mm^{-1}, min. and max. transmission factors 0.667 and 0.890; $2\theta_{max}$ = 56.64°; 21 325 collected reflections, 4929 unique [R_{int} = 0.052]; number of data/restraints/parameters 4929/5/257; final GoF 1.199; R_1 = 0.089 [4289 reflections, $I > 2\sigma(I)$]; wR_2 = 0.184 for all data; Flack parameter x = 0.06(10); largest difference peak 2.13 e Å^{-3} close to the metal atom with no chemical sense. The acetone solvent molecule shows static disorder but no clear model could be established, dynamic disorder has been assumed.

Acknowledgements

We thank the Ministerio de Educación y Ciencia (Grant CTQ 2009-10303/BQU and CONSOLIDER INGENIO-2010 program under the project Factoría de Cristalización, CSD2006-0015) and Gobierno de Aragón (Grupo Consolidado: Catalizadores Organometálicos Enantioselectivos) for financial support. P. G. O. acknowledges financial support from the CSIC, "*JAE-Doc*" program, contract co-funded by the ESF.

Notes and references

1 (*a*) *The Handbook of Homogeneous Hydrogenation*, ed. J. G. de Vries, Wiley-VCH, Weinheim, 2007, vol. 3, p. 1215; (*b*) *Comprehensive Asymmetric Catalysis, Suppl. 1 and 2*, ed. E. N. Jacobsen, A. Pfaltz and H. Yamamoto, Springer, Berlin, 2004; (*c*) *Asymmetric Catalysis on Industrial Scale*, ed. H. U. Blaser and E. Schmidt, Wiley-VCH, Weinheim, 2003; (*d*) R. Noyori and S. Hashiguchi, *Acc. Chem. Res.*, 1997, **30**, 97–102; (*e*) M. J. Palmer and M. Wills, *Tetrahedron: Asymmetry*, 1999, **10**, 2045–2061; (*f*) K. Everaere, A. Mortreaux and J. F. Carpentier, *Adv. Synth. Catal.*, 2003, **345**, 67–77; (*g*) S. E. Clapham, A. Hadzovic and R. H. Morris, *Coord. Chem. Rev.*, 2004, **248**, 2201–2237; (*h*) T. Ikariya, K. Murata and R. Noyori, *Org. Biomol. Chem.*, 2006, **4**, 393–406; (*i*) S. Gladiali and E. Alberico, *Chem. Soc. Rev.*, 2006, **35**, 226–236; (*j*) J. S. M. Samec, P. G. Bäckvall, P. G. Andersson and P. Brandt, *Chem. Soc. Rev.*, 2006, **35**, 237–248; (*k*) T. Ikariya and A. J. Blacker, *Acc. Chem. Res.*, 2007, **40**, 1300–1308; (*l*) C. Wang, X. Wu and J. Xiao, *Chem.–Asian J.*, 2008, **3**, 1750–1770; (*m*) T. Ikariya, *Bull. Chem. Soc. Jpn.*, 2011, **84**, 1–16.

2 (*a*) *Chirality in Industry II: Developments in the Manufacture and Applications of Optically Active Compounds*, ed. A. N. Collins, G. N. Sheldrake and J. Crosby, John Wiley & Sons, Chichester, 1997, p. 391; (*b*) *The Handbook of Homogeneous Hydrogenation*, ed. J. G. de Vries, Wiley-VCH, Weinheim, 2007, vol. 3, p. 1279.

3 (*a*) S. Hashiguchi, A. Fuji, J. Takehara, T. Ikariya and R. Noyori, *J. Am. Chem. Soc.*, 1995, **117**, 7562–7563; (*b*) A. Fuji, S. Hashiguchi, N. Uematsu, T. Ikariya and R. Noyori, *J. Am. Chem. Soc.*, 1996, **118**, 2521–2528.

4 (*a*) K. J. Haack, S. Hashiguchi, A. Fuji, T. Ikariya and R. Noyori, *Angew. Chem., Int. Ed. Engl.*, 1997, **36**, 285–288; (*b*) M. Yamakawa, H. Ito and R. Noyori, *J. Am. Chem. Soc.*, 2000, **122**, 1466–1478; (*c*) R. Noyori, M. Yamakawa and S. Hashiguchi, *J. Org. Chem.*, 2001, **66**, 7931–7944.

5 (*a*) R. Soni, J. M. Collinson, G. C. Clarkson and M. Wills, *Org. Lett.*, 2011, **13**, 4304–4307; (*b*) T. Touge, T. Hakamata, H. Nara, T. Kobayashi, Y. Ski, N. Sayo, T. Saito, Y. Kayaki and T. Ikariya, *J. Am. Chem. Soc.*, 2011, **133**, 14960–14963.

6 (*a*) M. Yamakawa, I. Yamada and R. Noyori, *Angew. Chem., Int. Ed.*, 2001, **40**, 2818–2821; (*b*) M. L. Han, X. P. Hu, J. D. Huang, L. G. Chen and Z. Zheng, *Tetrahedron: Asymmetry*, 2011, **22**, 222–225.

7 (*a*) F. W. Faller and A. R. Lavoie, *Organometallics*, 2001, **20**, 5245–5247; (*b*) Y. A. Rhyoo, H. J. Park, W. H. Suh and Y. K. Chung, *Tetrahedron Lett.*, 2002, **43**, 269–272; (*c*) W. Hoffmueller, H. Dialer and W. Beck, *Z. Naturforsch., B: Chem. Sci.*, 2005, **60**, 1278–1286; (*d*) A. S. Y. Yim and M. Wills, *Tetrahedron*, 2005, **61**, 7994–8004; (*e*) A. Bacchi, P. Pelagatti, C. Pelizzi and D. Rogolino, *J. Organomet. Chem.*, 2009, **694**, 3200–3211; (*f*) A. B. Zaitsev and H. Adolfsson, *Org. Lett.*, 2006, **8**, 5129–5132; (*g*) J. Wettergren, E. Buitrago, P. Ryberg and H. Adolfsson, *Chem.–Eur. J.*, 2009, **15**, 5709–5718; (*h*) H. Lundberg and H. Adolfsson, *Tetrahedron Lett.*, 2011, **52**, 2754–2758.

8 (*a*) A. A. Ioganson, *Russ. Chem. Rev.*, 1985, **54**, 277–292; (*b*) L. D. Pettit and M. Bezer, *Coord. Chem. Rev.*, 1985, **61**, 97–114; (*c*) S. H. Laurie, in *Comprehensive Coordination Chemistry*, ed. G. Wilkinson, Pergamon, Oxford, 1987, vol. 2, ch. 20.2, p. 739; (*d*) H. Kozlowski and L. D. Pettit, in *Chemistry of the Platinum Group Metals*, ed. F. R. Hartley, Elsevier, New York, 1991, ch. 15, p. 530; (*e*) N. Paulic and N. Raos, *J. Coord. Chem.*, 1994, **31**, 181–190; (*f*) A. Iakovidis and N. Hadjiliadis, *Coord. Chem. Rev.*, 1994, **135–136**, 17–63; (*g*) T. G. Appleton, *Coord. Chem. Rev.*, 1997, **166**, 313–359.

9 K. Severin, R. Bergs and W. Beck, *Angew. Chem., Int. Ed.*, 1998, **37**, 1634–1654 and references therein.

10 (*a*) K. Sünkel, W. Hoffmüller and W. Beck, *Z. Naturforsch., B: Chem. Sci.*, 1998, **53**, 1365–1368; (*b*) A. Bohm, K. Polborn and W. Beck, *Z. Naturforsch., B: Chem. Sci.*, 2001, **56**, 293–296; (*c*) K. Majumder and S. Bhattacharya, *Polyhedron*, 1999, **18**, 3669–3673; (*d*) P. Pelagatti, A. Bacchi, F. Calbiani, M. Carcelli, L. Elviri, C. Pelizzi and D. Rogolino, *J. Organomet. Chem.*, 2005, **690**, 4602–4610; (*e*) C. P. Roy, L. A. Huff, N. A. Barker, M. A. G. Berg and J. S. Merola, *J. Organomet. Chem.*, 2006, **691**, 2270–2276; (*f*) G. Ciancaleoni, I. Di Maio, D. Zuccaccia and A. Macchioni, *Organometallics*, 2007, **26**, 489–496.

11 (*a*) T. Ohta, S. Nakahara, Y. Shigemura, K. Hattori and I. Furukawa, *Chem. Lett.*, 1998, 491–492; (*b*) T. Ohta, S. Nakahara, Y. Shigemura, K. Hattori and I. Furukawa, *Appl. Organomet. Chem.*, 2001, **15**, 699–709.

12 (*a*) D. Carmona, A. Mendoza, F. J. Lahoz, L. A. Oro, M. P. Lamata and E. San José, *J. Organomet. Chem.*, 1990, **396**, C17–C21; (*b*) D. Carmona, F. J. Lahoz, R. Atencio, L. A. Oro, M. P. Lamata and E. San, *Tetrahedron: Asymmetry*, 1993, **4**, 1425–1428; (*c*) M. L. Jimeno, J. Elguero, D. Carmona, M. P. Lamata and E. San José, *Magn. Reson. Chem.*, 1996, **34**, 42–46; (*d*) D. Carmona, F. J. Lahoz, R. Atencio, L. A. Oro, M. P. Lamata, F. Viguri, E. San José, C. Vega, J. Reyes, F. Joó and A. Kathó, *Chem.–Eur. J.*, 1999, **5**, 1544–1564; (*e*) D. Carmona, C. Vega, F. J. Lahoz, R. Atencio, L. A. Oro, M. P. Lamata, F. Viguri and E. San José, *Organometallics*, 2000, **19**, 2273–2280; (*f*) A. Kathó, D. Carmona, F. Viguri, C. D. Remacha, J. Kovács, F. Joó and L. A. Oro, *J. Organomet. Chem.*, 2000, **593–594**, 299–306; (*g*) D. Carmona, M. P. Lamata, F. Viguri, I. T. Dobrinovich, F. J. Lahoz and L. A. Oro, *Adv. Synth. Catal.*, 2002, **344**, 499–502; (*h*) D. Carmona, M. P. Lamata and L. A. Oro, *Eur. J. Inorg. Chem.*, 2002, 2239–2251; (*i*) D. Carmona, F. J. Lahoz, P. García-Orduña, L. A. Oro, M. P. Lamata and F. Viguri, *Organometallics*, 2012, **31**, 3333–3345.

13 M. A. Bennett, T. R. B. Mitchell, M. R. Stevens and A. C. Willis, *Can. J. Chem.*, 2001, **79**, 655–669.

14 W. S. Sheldrick, E. Hauck and S. Korn, *J. Organomet. Chem.*, 1994, **467**, 283–292.

15 R. Atencio, Ph.D. Thesis, University of Zaragoza, 1995.

16 C. J. Jones, J. A. McCleverty and A. S. Rothin, *J. Chem. Soc., Dalton Trans.*, 1986, 109–111.

17 (*a*) S. H. Laurie, in *Comprehensive Coordination Chemistry*, ed. G. Wilkinson, Pergamon, Oxford, 1987, vol. 2, ch, 22, p. 964; (*b*) K. Nakamoto, *Infrared and Raman Spectra of Inorganic and Coordination Compounds*, 4th edn, Wiley-Interscience, New York, 1986, p. 233.

18 Ligand priority sequence *p*-MeC$_6$H$_4$iPr > Cl > O > N: (*a*) R. S. Cahn, C. Ingold and V. Prelog, *Angew. Chem., Int. Ed. Engl.*, 1966, **5**, 385–415; (*b*) V. Prelog and G. Helmchen, *Angew. Chem., Int. Ed. Engl.*, 1982, **21**, 567–583; (*c*) C. Lecomte, Y. Dusausoy, J. Protas and J. Tirouflet, *J. Organomet. Chem.*, 1974, **73**, 67–76; (*d*) K. Stanley and M. C. Baird, *J. Am. Chem. Soc.*, 1975, **97**, 6598–6599; (*e*) T. E. Sloan, *Top. Stereochem.*, 1981, **12**, 1.

19 (*a*) R. Krämer, K. Polborn, H. Wanjek, I. Zahn and W. Beck, *Chem. Ber.*, 1990, **123**, 767–778; (*b*) W. S. Sheldrick and S. Heeb, *Inorg. Chim. Acta*, 1990, **168**, 93–100; (*c*) L. C. Carter, D. L. Davies, K. T. Duffy, J. Fawcett and D. R. Russell, *Acta Crystallogr., Sect. C: Cryst. Struct. Commun.*, 1994, **50**, 1559–1561; (*d*) H. Brunner, M. Weber and M. Zabel, *Coord. Chem. Rev.*, 2003, **242**, 3–13; (*e*) D. Carmona, C. Vega, N. García, F. J. Lahoz, S. Elipe, L. A. Oro, M. P. Lamata, F. Viguri and R. Borao, *Organometallics*, 2006, **25**, 1592–1606.

20 D. Cremer and J. A. Pople, *J. Am. Chem. Soc.*, 1975, **97**, 1354–1358.

21 J. Yan, X. L. Lu, J. D. Lou, L. Zhang, P. S. Nong, Y. L. Feng, M. Gao and J. J. Yang, *Synth. React. Inorg., Met.-Org., Nano-Met. Chem.*, 2011, **41**, 26–30.
22 (*a*) R. Krämer, K. Polborn, C. Robl and W. Beck, *Inorg. Chim. Acta*, 1992, **198–200**, 415–420; (*b*) S. Ogo, H. Chen, M. M. Olmstead and R. H. Fish, *Organometallics*, 1996, **15**, 2009–2013.
23 Ligand priority sequence[18] *p*-MeC_6H_4iPr > O(chelate) > O(bridging) > N.
24 Assignment of the *pro-S* and *pro-R* NCH_2 resonances was made through inspection of their NOE effects with the NH proton.
25 W. Li, G. Hou, C. Wang, Y. Jiang and X. Zhang, *Chem. Commun.*, 2010, **46**, 3979–3981.
26 *SAINT+, version 6.01*, Bruker AXS, Inc, Madison, WI, 2001.
27 G. M. Sheldrick, *Acta Crystallogr., Sect. A: Found. Crystallogr.*, 1997, **46**, 467–473.
28 G. M. Sheldrick, *Acta Crystallogr., Sect. A: Found. Crystallogr.*, 2008, **64**, 112–122.
29 H. D. Flack, *Acta Crystallogr., Sect. A: Found. Crystallogr.*, 2008, **39**, 876–881.

